# Spatial Oversampling for Quantized LoS MIMO

Ahmet Dundar Sezer, Upamanyu Madhow, and Mark J. W. Rodwell
Department of Electrical and Computer Engineering
University of California, Santa Barbara
Santa Barbara, California 93106
Email: {adsezer, madhow, rodwell}@ece.ucsb.edu

2021 55th Asilomar Conference on Signals, Systems, and Computers | 978-1-6654-5828-3/21/$31.00 ©2021 IEEE | DOI: 10.1109/IEEECONF53345.2021.9723314

***Abstract*—Line of sight (LoS) multi-input multi-output (MIMO) systems provide attractive scaling properties for emerging millimeter wave (mmWave) systems, with the number of spatial degrees of freedom and available bandwidth both scaling up with carrier frequency. A standard architecture for LoS MIMO is an array of subarrays, where the number of subarrays equals the number of available spatial degrees of freedom. While this has the advantage of permitting each subarray to employ radio frequency (RF) beamforming, recent developments in mmWave radio frequency integrated circuits (RFICs) motivate consideration of more flexible configurations employing a larger number of receive antennas, with each element having its own RF chain and digital output. In this paper, we investigate how spatial oversampling with such configurations can help relax precision requirements for analog-to-digital converters (ADCs), which is a significant challenge as signaling bandwidths scale up. We illustrate our ideas via LoS MIMO systems with 4 spatially multiplexed QPSK and 16QAM modulated data streams and 2/3/4-bit ADCs, showing that 16 receive antenna elements spaced evenly across the aperture outperform standard array of subarrays architectures with the same number of antenna elements.**

## I. Introduction

Line of sight (LoS) multi-input multi-output (MIMO) systems in emerging mmWave bands have attractive scaling properties as the carrier frequency increases: for a fixed form factor and link range, the available spatial degrees of freedom increase linearly and quadratically for 1D and 2D arrays, respectively, and the available signaling bandwidth typically increases linearly, with carrier frequency. For example, 4-fold spatial multiplexing in a 140 GHz system with 20 GHz signaling bandwidth, QPSK signaling, and 100 meters range achieves a data rate of 160 Gbps (approaching that of optical links) while requiring transmit and receive apertures of size 0.69 meters for a 1D array, and 0.11 square meters for a 2D array. A standard architecture for such systems is an array of subarrays [1], with the number of subarrays equal to the number of spatial degrees of freedom. The advantage of such an architecture is that each transmit or receive subarray can perform RF beamforming, which requires a single RF chain per subarray. In order to provide flexibility in baseband processing for spatial demultiplexing, we would like to employ digital processing at the subarray outputs. This requires analog-to-digital converters (ADCs) for each subarray output. A fundamental bottleneck to scaling then becomes the relatively low ADC precision available as signaling bandwidth increases.

With the emergence of radio frequency integrated circuits (RFICs) at 100+ GHz supporting all-digital MIMO, with one RF chain for each antenna [2], [3], it becomes possible to explore more flexible antenna configurations. In this paper, we provide detailed results indicating that spacing out receive antennas across the aperture has the potential for alleviating the performance bottleneck imposed by low ADC precision. We consider an LoS MIMO system with four spatially multiplexed QPSK (16QAM) streams, with 16 antennas and 2-bit (4-bit) ADCs available at the receiver, and compare three configurations:

(a) a benchmark $4 \times 4$ array of subarrays architecture with 4 receive subarrays, each with 4 elements. We assume RF beamforming at each subarray to eliminate quantization loss, and apply the ADCs to each subarray output. In this case, we have 4 digital outputs.

(b) a $4 \times 8$ system in which 8 receive subarrays are evenly spaced across the aperture, each subarray containing 2 elements employing RF beamforming. This results in 8 digital outputs.

(c) a $4 \times 16$ system with 16 digital outputs from 16 elements evenly spaced across the aperture.

We do not employ transmit precoding. Note that the received SNR per data stream prior to ADC is the same across the configurations. We show that, under the drastically reduced precision considered here, spatial oversampling in the $4 \times 16$ system yields substantially better performance than the classical $4 \times 4$ array of subarrays architecture.

**Related work:** The degrees of freedom available in LoS MIMO systems have been well-studied in the literature [1], [4]. The standard architecture for attaining these degrees of freedom is an array of subarrays, where the number of subarrays equals the number of spatially multiplexed streams. The outputs from the subarrays are then spatially demultiplexed. Recent efforts in the research literature have focused on analog-centric [5], [6] or hybrid analog-digital [7], [8] processing for spatial demultiplexing in array of subarrays architectures. mmWave LoS MIMO links deployed in the field by industry (e.g., [9]) also employ an array of subarrays, where the "subarrays" tend to be fixed, highly directive antennas. Recent study in [10] shows that all-digital processing in LoS MIMO receivers with severely quantized samples is possible for an array of subarrays architectures, introducing the concept of *virtual quantization* which trades increased complexity in digital processing for reducing ADC hardware complexity.

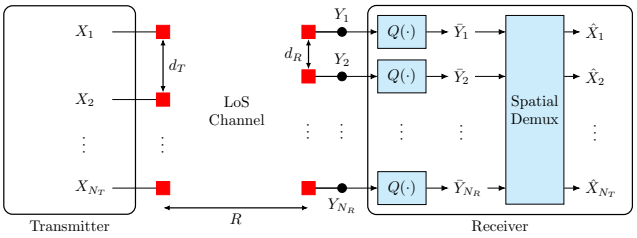


Fig. 1. Spatially oversampled LoS MIMO communication system model

However, this approach still incurs an error floor for severely quantized observations.

Like [10], we also consider all-digital LoS MIMO with low ADC precision. However, we seek to reduce signal processing complexity and improve performance by departing from the standard array of subarrays architecture considered in the preceding papers. Our approach is based on the recognition that, as it becomes more feasible to increase the number of RF chains in an all-digital architecture, there is an opportunity to spread out the antennas without increasing the RF hardware complexity. This provides a number of received digital streams that exceeds the number of spatially multiplexed streams, and we show that such spatial oversampling helps mitigate the impact of drastic quantization. We note that relatively large apertures and antenna spacings are required to create spatial degrees of freedom in an LoS setting, hence it is possible to add antennas to the aperture without increasing the form factor.

Spatial oversampling has been employed previously to mitigate the frequency selectivity caused by geometric misalignments in LoS MIMO [11], but quantization constraints were not considered there. To the best of our knowledge, the present paper is the first to explore the potential for alleviating the ADC bottleneck using spatial oversampling.

## II. System Model

Consider a $N_T \times N_R$ LoS MIMO communication scheme in which a $N_T$-antenna transmitter with inter-antenna spacing of $d_T$ and a receiver having $N_R$ units with inter-unit spacing of $d_R$, both having the same aperture (i.e., $(N_T-1)d_T = (N_R-1)d_R$), are aligned with horizontal distance of $R$ as represented in Fig. 1. Assuming each transmit/receive antenna produces a highly directive beam along the LoS, multipath is ignored. We consider the same aperture (i.e., form factor) for both the transmitter and the receiver. For given $N_T$, we set the inter-antenna spacing of the transmit antennas to

$$d_T = \sqrt{\frac{\lambda R}{N_T}} \tag{1}$$

We allow $N_R$ to vary, and set

$$d_R = \frac{d_T(N_T-1)}{N_R-1}\,. \tag{2}$$

Based on the given model in Fig. 1, the received signal vector $\mathbf{Y} \triangleq [Y_1 \cdots Y_{N_R}]^\mathsf{T} \in \mathbb{C}^{N_R \times 1}$ is given by

$$\mathbf{Y} = \mathbf{H}\,\mathbf{X} + \mathbf{N}\,, \tag{3}$$

where $\mathbf{X} \triangleq [X_1 \cdots X_{N_T}]^\mathsf{T} \in \mathbb{C}^{N_T \times 1}$ is the transmitted symbol vector, $\mathbf{H} \in \mathbb{C}^{N_R \times N_T}$ is the normalized channel matrix, and $\mathbf{N} \sim \mathcal{CN}(0, \sigma^2\,\mathbf{I}_{N_R})$ is AWGN.

Given $R \gg (N_T-1)d_T = (N_R-1)d_R$, the path loss differences among the transmit-receive pairs can be ignored and the channel between transmit element $n$ and receive unit $m$ is given by

$$\mathbf{H}(m,n) = \sqrt{N_A}\, e^{-j\Phi}\, e^{-j\theta_{m,n}}\,, \tag{4}$$

where $N_A$ denotes the number of antenna elements at each receive unit (i.e., subarray), the random variable $\Phi$ denotes the common phase change along the path between the transmitter and the receiver and is assumed to be uniformly distributed over $[0, 2\pi)$, and

$$\theta_{m,n} \approx \frac{\pi((n-1)d_T - (m-1)d_R)^2}{\lambda R}, \tag{5}$$

for $R \gg (N_T-1)d_T = (N_R-1)d_R$ with $\lambda$ denoting the carrier wavelength.

**Input:** We consider QPSK and 16QAM modulations. For all modulations, $\{X_i\}_{i=1}^{N_T}$ are independent and identically distributed symbols taking values from the corresponding signaling constellation with equal probability. In our simulations, we define the average SNR per receive element/antenna as $SNR = \mathbb{E}\{|X_k|^2\}/(\sigma^2) = 1/(\sigma^2)$ where $\mathbb{E}\{|X_k|^2\} = 1$ for all $k \in \{1, \ldots, N_T\}$, which is considered as SISO SNR. We note that the SNR per receive unit does scale with the number of elements per unit (i.e., $N_A$), which corresponds to the analog beamforming gain ($N_A$-fold increase) at each receive unit (i.e., subarray).

**Quantizer:** We consider identical regular I/Q quantizers at each subarray, or receive unit. Mathematically, the quantized output of the $i$th receive unit can be expressed as

$$\bar{Y}_i = Q(Y_i)\,, \tag{6}$$

for $i \in \{1, \ldots, N_R\}$, where $Q(\cdot)$ represents the quantizer function at each receive unit.

We consider b-bit I/Q quantization scheme with $S^2$ regions (i.e., $S = 2^b$), for which the quantization set of $(j+S(i-1))$th-bin can be written as

$$\Gamma_{j+S(i-1)} = \{Y \mid I_{i-1} \le \Re(Y) < I_i\,, \quad Q_{j-1} \le \Im(Y) < Q_j\}\,, \tag{7}$$

for $i, j \in \{1, \ldots, S\}$, where $I_1, \ldots, I_{S-1}$ and $Q_1, \ldots, Q_{S-1}$ are the thresholds for in-phase and quadrature, respectively. We set $I_0 = -\infty$, $I_S = \infty$, $Q_0 = -\infty$, and $Q_S = \infty$. Then, for a given input $y$, $Q(y)$ can be characterized as

$$Q(y) = \tilde{y}_j\,, \text{ if } \; y \in \Gamma_j\,, \tag{8}$$

for $j \in \{1, \ldots, S^2\}$, where $\tilde{y}_j$ for $j \in \{1, \ldots, S^2\}$ corresponds to the quantizer output and $\Gamma_1$, …, $\Gamma_{S^2}$ denote the decision regions for the quantizer.

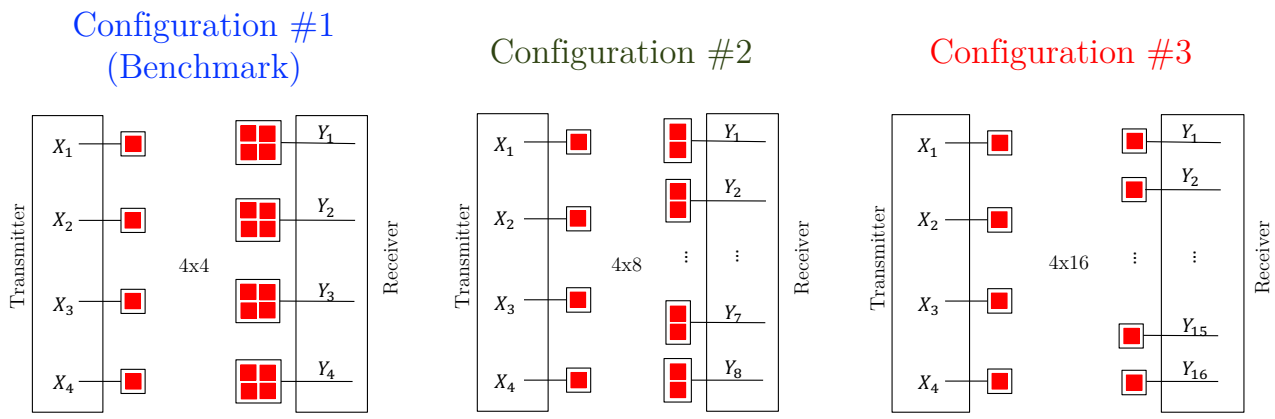


Fig. 2. Three configurations: (Left) $4 \times 4$ array of subarray architecture and our proposed (Middle) $4 \times 8$ and (Right) $4 \times 16$ systems with spatial oversampling

As in [12], for drastic quantization, we find it advantageous to employ entropy-maximizing quantizer thresholds rather than classical minimum mean squared error (MMSE) quantization. Therefore, the entropy-maximizer thresholds based on a Gaussian approximation of the unquantized outputs are calculated as

$$I_i = Q_i = \sqrt{\frac{4N_A + \sigma^2}{2}} \Phi^{-1}\left(\frac{i}{S}\right) \tag{9}$$

for $i \in \{1, \ldots, S-1\}$, where $\Phi^{-1}$ is the inverse distribution function for the standard Gaussian distribution with a mean of 0 and a standard deviation of 1.

**Spatial demultiplexer:** Maximum likelihood detection based on quantized observations is intractable, hence we employ linear ZF detection for spatial demultiplexing, setting the quantizer outputs to the centroids of the corresponding quantizer regions. The linear ZF solution can be obtained by first computing

$$\tilde{\mathbf{X}}(\mathbf{Y}_Q) = (\mathbf{H}^\dagger \mathbf{H})^{-1} \mathbf{H}^\dagger \mathbf{Y}_Q \,, \tag{10}$$

where $\mathbf{Y}_Q \triangleq \left[\bar{Y}_1 \cdots \bar{Y}_{N_R}\right]^\intercal$ and then projecting the elements of $\tilde{\mathbf{X}}(\mathbf{Y}_Q)$ onto the constellation symbols.

## III. Results and Discussion

We consider the following scenarios in our performance evaluation: a transmitter with $N_T = 4$ antennas communicates with a receiver with $N_R \in \{4, 8, 16\}$ receive units, each having $N_A = 16/N_R$ receive antennas. Those three configurations are presented in Fig. 2.

Although our focus is on demultiplexing with severely quantized observations, we first consider the unquantized scenario where ADCs at the receivers are assumed to have infinite precision. For those configurations in Fig. 2, Fig. 3 plots BER averaged over the common phase $\Phi$ versus SNR for QPSK modulation as if there is no quantization performed at the receivers. As expected, the benchmark $4 \times 4$ array of subarrays architecture with 4 receive subarrays at Rayleigh spacing [1] is optimal for the considered unquantized scenario since the received responses for the 4 transmitted streams are orthogonal and the unquantized SNRs across the three systems are equal. Our proposed $4 \times 16$ system with 16 elements evenly spaced across the aperture requires 1 dB higher SNR compared to the benchmark $4 \times 4$ system to achieve the same BER performance.

We now turn to the scenario of interest for us and factor in the severe quantization at the receivers with low-precision ADCs for which spatial oversampling provides advantage. For 2 bit I/Q quantization, Fig. 4 plots BER averaged over the common phase $\Phi$ versus SNR for these configurations with QPSK modulation. We see from the figure that under the drastic 2 bit quantization that we consider, both the $4 \times 8$ and $4 \times 16$ systems perform better than the $4 \times 4$ system which exhibits an error floor that stays higher than $10^{-3}$ BER. Our proposed $4 \times 16$ system with spatial oversampling achieves $10^{-4}$ BER at 10 dB SNR, which is quite sufficient to achieve reliable communication with high-rate error correcting codes. Note that we have assumed that the $4 \times 4$ system does not

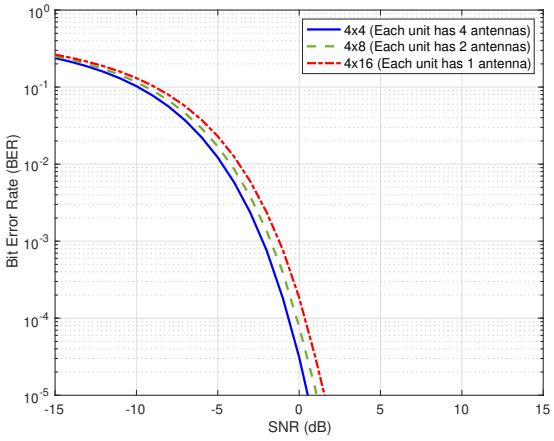


Fig. 3. QPSK with unquantized observations (BER vs. SNR)

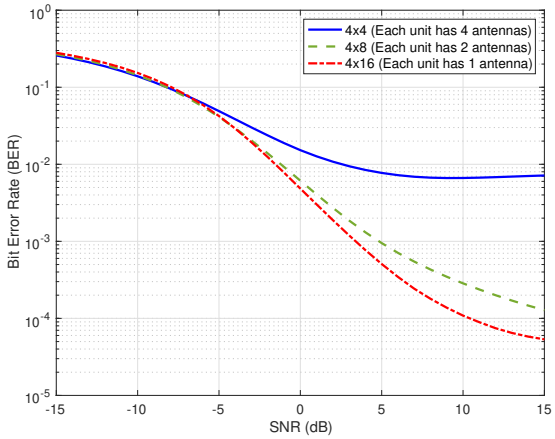


Fig. 4. QPSK with 2-bit I/Q quantization (BER vs. SNR)

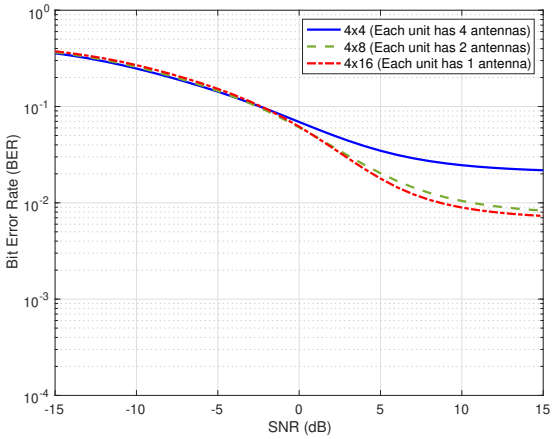


Fig. 6. 16QAM with 3-bit I/Q quantization (BER vs. SNR)

suffer quantization loss for beamforming by each subarray. For truly all-digital LoS MIMO, in which RF beamforming without quantization loss is not possible for a standard array of subarrays configuration, the performance loss relative to spatial oversampling is expected to be even larger.

Next, we investigate how the considered configurations perform when we increase the precision of quantization 1 bit. For that reason, we plot BER averaged over the common phase $\Phi$ versus SNR in Fig. 5 for 3 bit I/Q quantization with QPSK. Fig. 5 shows that all three configurations achieve similar BER performance under 3 bit I/Q quantization. Also, given the lower dynamic range of QPSK, none of the configurations exhibits error floor at high SNR. However, it is important to emphasize that the linear increase in the number of quantization bits causes an exponential increase in the complexity of ADC design. Also, this conflicts with our aim in this study which is to reduce precision requirements for ADCs.

We now consider the higher order modulation and evaluate the performance of our configurations for 16QAM. Given the higher dynamic range of 16QAM, it is obvious that 2-bit I/Q quantization is not sufficient for the system with 16QAM to achieve adequate BER performance. Therefore, we consider 3 bit and 4 bit I/Q quantization for 16QAM. For three configurations with 16QAM, Fig. 6 and Fig. 7 plot BER averaged over the common phase $\Phi$ versus SNR for 3 bit and 4 bit I/Q quantization, respectively. In Fig. 6, we see that neither of these configurations can achieve $10^{-3}$ BER even at high SNR when 3 bit I/Q quantization is employed at the receivers. On the other hand, we observe from Fig. 7 that under 4 bit I/Q quantization, our proposed $4 \times 8$ and $4 \times 16$ systems outperform the $4 \times 4$ array of subarrays architecture. The $4 \times 4$ array of subarrays architecture cannot achieve $10^{-3}$ BER at

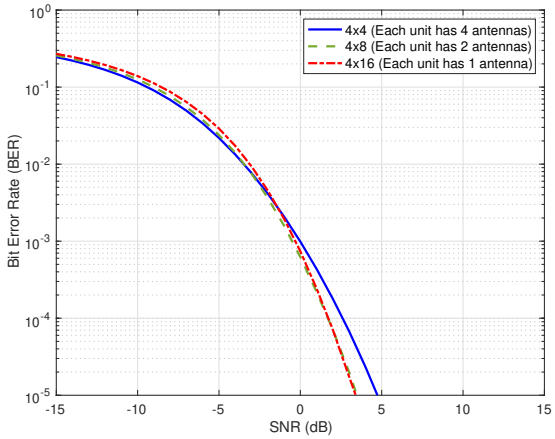


Fig. 5. QPSK with 3-bit I/Q quantization (BER vs. SNR)

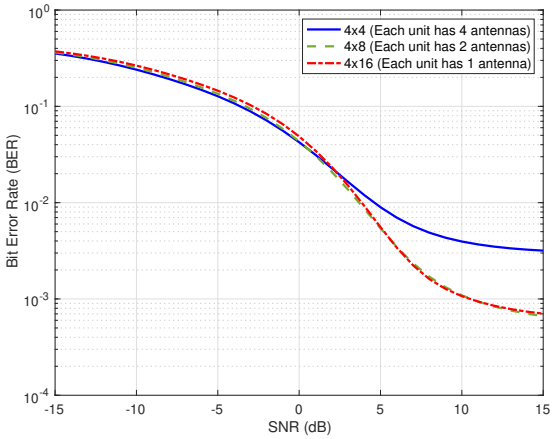


Fig. 7. 16QAM with 4-bit I/Q quantization (BER vs. SNR)

high SNR, whereas both of our $4 \times 8$ and $4 \times 16$ systems achieve $10^{-3}$ BER at 10 dB SNR.

## IV. Conclusion

Our study of spatial oversampling for LoS MIMO has shown that precision requirements for ADCs can be reduced by spacing out receive antennas across the aperture. We show that our proposed $4 \times 16$ system with spatial oversampling defeats the benchmark $4 \times 4$ array of subarrays architecture when 2 bit I/Q quantization is considered for QPSK and 4 bit I/Q quantization is considered for 16QAM. An important future research direction is to investigate how far we can push the concept of spatial oversampling to reduce the precision requirements for ADCs (e.g., down to 1 bit), developing analytical guidelines for system design in the presence of severe nonlinearities analogous to those recently developed for multiuser MIMO systems [13]. As noted in the introduction, for unquantized systems, spatial oversampling has also been shown to be effective in combating channel dispersion due to geometric misalignments [11]. These prior results, together with the results discussed here, point to the promise of spatial oversampling as a powerful tool for robustness against a variety of impairments. Although we do not employ transmit precoding in this study, joint transmit-receive optimization to reduce transceiver complexity is an important direction to examine.

## Acknowledgment

This work was supported in part by ComSenTer, one of six centers in JUMP, a Semiconductor Research Corporation (SRC) program sponsored by DARPA. Use was made of computational facilities purchased with funds from the National Science Foundation (CNS-1725797) and administered by the Center for Scientific Computing (CSC). The CSC is supported by the California NanoSystems Institute and the Materials Research Science and Engineering Center (MRSEC; NSF DMR 1720256) at UC Santa Barbara.

## References

[1] E. Torkildson, U. Madhow, and M. Rodwell, "Indoor millimeter wave MIMO: Feasibility and performance," *IEEE Transactions on Wireless Communications*, vol. 10, no. 12, pp. 4150–4160, Dec. 2011.

[2] A. Simsek, S.-K. Kim, and M. J. Rodwell, "A 140 ghz MIMO transceiver in 45 nm SOI CMOS," in *2018 IEEE BiCMOS and Compound Semiconductor Integrated Circuits and Technology Symposium (BCICTS)*, 2018, pp. 231–234.

[3] A. A. Farid, A. Simsek, A. S. H. Ahmed, and M. J. W. Rodwell, "A broadband direct conversion transmitter/receiver at d-band using CMOS 22nm FDSOI," in *2019 IEEE Radio Frequency Integrated Circuits Symposium (RFIC)*, 2019, pp. 135–138.

[4] F. Bohagen, P. Orten, and G. E. Oien, "Design of optimal high-rank line-of-sight MIMO channels," *IEEE Transactions on Wireless Communications*, vol. 6, no. 4, pp. 1420–1425, 2007.

[5] M. Sawaby, B. Mamandipoor, U. Madhow, and A. Arbabian, "Analog processing to enable scalable high-throughput mm-Wave wireless fiber systems," in *50th Asilomar Conference on Signals, Systems and Computers*, Nov. 2016, pp. 1658–1662.

[6] Y. Yan, P. Bondalapati, A. Tiwari, C. Xia, A. Cashion, D. Zhang, Q. Tang, and M. Reed, "11-Gbps broadband modem-agnostic line-of-sight MIMO over the range of 13 km," in *IEEE Global Communications Conference (GLOBECOM)*, 2018, pp. 1–7.

[7] A. Khalili, S. Rini, L. Barletta, E. Erkip, and Y. C. Eldar, "On MIMO channel capacity with output quantization constraints," in *IEEE International Symposium on Information Theory (ISIT)*, June 2018, pp. 1355–1359.

[8] L. Zhu, S. Wang, and J. Zhu, "Adaptive beamforming design for millimeter-wave line-of-sight MIMO channel," *IEEE Communications Letters*, vol. 23, no. 11, pp. 2095–2098, 2019.

[9] Ericsson Press Release, "Deutsche Telekom and Ericsson top 100Gbps over microwave link," May 2019. [Online]. Available: https://www.ericsson.com/en/press-releases/2019/5/deutsche-telekom-and-ericsson-top-100gbps-over-microwave-link

[10] A. D. Sezer and U. Madhow, "All-digital LoS MIMO with low-precision analog-to-digital conversion," 2021.

[11] P. Raviteja and U. Madhow, "Spatially oversampled demultiplexing in mmWave LoS MIMO," in *IEEE 19th International Workshop on Signal Processing Advances in Wireless Communications (SPAWC)*, June 2018, pp. 1–5.

[12] A. D. Sezer and U. Madhow, "Near-optimal quantization for LoS MIMO with QPSK modulation," in *53rd Asilomar Conference on Signals, Systems, and Computers*, 2019, pp. 1015–1020.

[13] M. Abdelghany, A. A. Farid, M. E. Rasekh, U. Madhow, and M. J. W. Rodwell, "A design framework for all-digital mmWave massive MIMO with per-antenna nonlinearities," *IEEE Transactions on Wireless Communications*, vol. 20, no. 9, pp. 5689–5701, 2021.